

ASSESSMENT OF NUMERICAL UNCERTAINTY FOR THE CALCULATIONS OF TURBULENT FLOW OVER A BACKWARD FACING STEP

Ismail B. Celik and Jun Li
Mechanical and Aerospace Engineering Department
West Virginia University, Morgantown, WV 26505 USA

ABSTRACT

Numerical uncertainty analysis has been performed for the turbulent flow past a backward facing step. The analysis is based on calculations on seven non-rectangular, but structured, grid sets that were provided by the organizers of the 2004 Lisbon Workshop. The calculations were performed by using a commercial code, namely, FLUENT with the Spalart-Allmaras' one-equation turbulence model. Since there was no experimental data made available, the present study constitutes simply a calculation verification process where by a set of partial differential equations are solved on gradually refined grid sets, and then the overall numerical uncertainty in selected quantities is estimated by various methods.

Some new ideas are presented for estimating the coefficient of variation, which is related to standard deviation (or standard error of estimate in case of least squares method).

The major problem that stands out again is the case of oscillatory convergence. For such case some alternative methods are proposed, and the results are assessed by comparing different methods with each other. Another issue that can not be ignored is the problem of interpolation to obtain the values of a selected parameter at a given spatial location from the results of calculations on different grids. The interpolation error could sometime overshadow the discretization error, and the remedy to this problem is not trivial.

BACKGROUND

The numerical uncertainty assessment is necessary for CFD (Computational Fluid Dynamics) to become a reliable design tool. Many of the approaches proposed in the literature for quantification of the numerical uncertainty are based on grid refinement in conjunction with Richardson extrapolation (RE) (Richardson 1910, 1927; Roache, 1998).

RE usually uses calculations on 3 sets of grids to determine the extrapolated value of a dependent variable to zero grid size, either using the theoretical order of the scheme (on at least two grid levels), or via the apparent or observed order which is calculated as part of the unknowns; in the latter case at least three sets of calculations are needed on significantly different grid levels. The pros and cons of this method has been the topic of many recent publications (Celik et al. (1993), Celik & Zhang (1993), Celik & Karatekin (1997), Roache (1998), Stern et al. (2001), Cadafalch et al. (2002), Eca & Hoekstra (2002)). In spite of being a very useful tool for quantifying discretization errors in CFD, there still remain major problems that need to be addressed to advance the level of confidence that could be trusted upon this method (Eca & Hoekstra 2003, Celik et al., 2004).

Alternative methods are proposed due to the difficulties of Richardson extrapolation. For instance, least squares approach is proposed to avoid the scattering of the data although it needs more than 3 sets of grids. AES (Approximate Error Spline) method (Celik et al. 2004) is proposed to solve the oscillatory convergence problems.

The organizers of the Lisbon workshop (Eca et al., 2004) have recognized the need for further refinement and assessment of the methods used for quantifying numerical uncertainty. This paper presents our findings from a careful study of numerical uncertainty for one of the test cases proposed by Eca et al. (2004). This is the classical case of a turbulent flow over a backward facing step. Our study will address on the following questions: (1) what is the effect of interpolation methods on the extrapolation? (2) Which extrapolation method is suitable for oscillatory convergence? (3) Which uncertainty estimation method is a better indicator for grid convergence? (4) How can the error estimates calculated from extrapolated values be translated into a quantitative uncertainty?

METHODS

With more than 3 sets of grids, we can use least squares method for extrapolation of computed quantities (Eca and Hoekstra, 2003). With 3 sets of grids, the following methods -- power law method, cubic spline method, polynomial, and Approximate Error Spline (AES) method are used in this study (See the appendix for the details of these methods; see also Celik et al., 2004 for more details). We use non-linear least squares extrapolation (see appendix A) with 4 and 7 sets of grids. In these cases the mean, μ , is simply taken as the extrapolated value, ϕ_{ext} . Once ϕ_{ext} is known the numerical uncertainty is calculated using the fine Grid Convergence Index (GCI) proposed by Roache (1998) which can be written as

$$U_{\phi}^f = 1.25 \left| \frac{\phi_{ext} - \phi_f}{\phi_f} \right| \quad (1)$$

An alternative way to estimate the uncertainty is to calculate the coefficient of variation. In this study, the coefficient of variation (CV) for the least squares method are computed from

$$\sigma_r = \sum_{i=1}^n [\phi_i - (\phi_{ext} + \alpha h_i^p)] \quad (2a)$$

$$\sigma_{\phi/h} = \sqrt{\sigma_r / (n-3)} \quad (2b)$$

$$CV = \left| \frac{\sigma_{\phi/h}}{\mu} \right| \quad (2c)$$

Here, $\mu = \phi_{ext}$ and ϕ_{ext} is equivalent to ϕ_0 in the appendix. σ_r is the sum of squares of the errors between the nonlinear regression line and the data points. $\sigma_{\phi/h}$ is the standard error of the fit. The coefficient of variation is the relative error of estimate.

For these methods requiring 3 sets of grids, the coefficient of variation is calculated from the sampling results with 4 triplets; Four sets of grids are denoted by G1, G2,G3, &G4, the sample size $n=4$, and the triplets are (G1,G2,G3); (G1,G3,G4); (G1,G2,G4) &(G2,G3,G4). Using these samples the mean μ is given by

$$\mu = \sum_{i=1}^n \phi_{ext,i} / n \quad (3a)$$

and the standard deviation is given by

$$\sigma = \sqrt{\sum_{i=1}^n (\phi_{ext,i} - \mu)^2 / (n-1)} \quad (3b)$$

The coefficient of variation is computed from

$$CV = \left| \frac{\sigma}{\mu} \right| \quad (3c)$$

Combining different methods of extrapolation, larger samples can be obtained to improve the statistics.

CASES AND SPECIFIC ISSUES

The case investigated in this study is a 2D turbulent backward facing step flow. The Reynolds number is 50,000 based on the step height and the maximum inlet velocity. The Expansion ration is 9/8. An example of seven sets of similar, structured, and non-Cartesian grids used in this study is shown in Figure 1. These grids are refined from 101*101 to 241*241. The averaged grid size is calculated from $h = \sqrt{A/n_c}$ where A is the area of the domain and n_c is the number of the cells. The grid refinement ratios for all these grids are in the range of 1.1~1.2 as listed in the first two columns of Table 1. These grids are used to estimate the numerical uncertainty with the least squares method. In this study we also selected some triplets to assess those extrapolation methods which are applicable for three sets of grids. For these triplets, the refinement ratios are in the range of 1.29~ 1.43 which is generally believed to be more appropriate in grid convergence study with three sets of grids. Four sets of grids listed in the last two columns of table 1 are also used to estimate the uncertainty with the least squares method and the results are compared to the ones that involved all seven sets of grids.

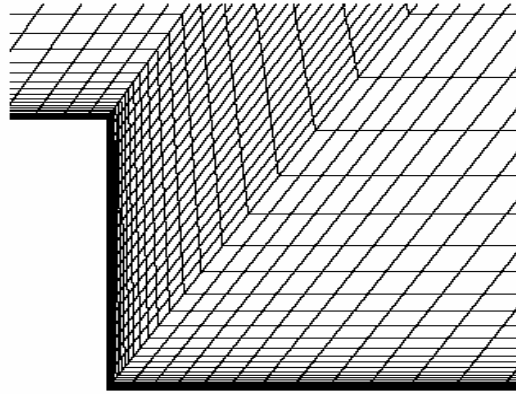


Figure 1 an example of grids used in this study

Table 1 Grid refinement ratios

grids	ratio		grids	Ratio		Grids	Ratio		grids	ratio
101*101			101*101			141*141			101*101	
121*121	1.20		141*141	1.40		181*181	1.29		141*141	1.40
141*141	1.17		201*201	1.43		241*241	1.33		181*181	1.29
161*161	1.14								241*241	1.33
181*181	1.13									
201*201	1.11									
241*241	1.20									

Sparlart-Allmaras' one-equation turbulence model is used to solve for the flow field with the commercial code FLUENT 6.0 (FLUENT CO. 2004). The convection terms and the diffusion terms are discretized with the second order upwinding scheme and the central differencing scheme, respectively. The inlet velocity is provided by Eca (2004). At the outlet, the gauge pressure and the derivatives of other quantities are set to be zero. The non-slip wall boundary condition is used at the walls. The shear stress at walls is obtained from laminar stress-strain relationship $u/u_\tau = \rho u_\tau y / \mu$.

For post-processing of the data, the bilinear interpolation method based on the quantities at four nodes of a cell is used with an order of accuracy in the range $1 < p < 2$. Interpolation methods with higher order are possible but they need also the quantities from neighboring cells. As a comparison, the results with quadratic interpolation method are also calculated to access the impact of interpolation errors. The quadratic interpolation method needs 6 nodes, two of which are from the neighboring cells. In this study,

for a cell with four nodes -- (x_i, y_i) , (x_i, y_{i+1}) , (x_{i+1}, y_i) , and (x_{i+1}, y_{i+1}) , we add two neighboring nodes (x_i, y_{i+2}) and (x_{i+2}, y_i) to build a linear system to solve the interpolation coefficients. It is worth to note here that selecting other nodes may result in a singular linear system of equations. For instance, choosing (x_i, y_{i+2}) and (x_{i+1}, y_{i+2}) will lead to singularity. Figure 2 shows us the streamwise velocities interpolated with the bilinear and quadratic interpolation methods along a vertical line at $x/H=3.0$ (H is the step height). The difference is not negligible especially in the recirculation region. Since the node choice for the quadratic interpolation method is not unique, we use the bilinear interpolation method for the calculations presented later to preserve the consistency. To study the influence of interpolation method further, 4 sets of rectangular grids are generated by doubling the grids. The results with these grids did not need any interpolation.

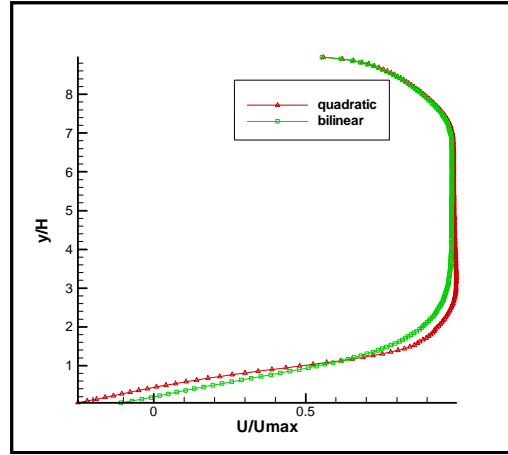


Figure 2 Interpolated streamwise velocity at $x=3.0$ with 101×101 grids

Double precision is used for all the calculations in this study. The machine accuracy for double precision is approximately $2.22E-16$ so that the round-off error is expected to be negligible. The iterations were stopped whenever the scaled residual for continuity equation approached an asymptotic value. The scaled residual is defined as

$$R^\phi = \frac{\sum_{cells\ p} \sum_{nb} |(a_{nb}\phi_{nb} + b - a_p\phi_p)|}{\sum_{cells\ p} |a_p\phi_p|} \quad (4)$$

Here a_p is the center coefficient of the discretization equation, a_{nb} are the influence coefficients for the neighboring cells, and b is the contribution of the source term. Correspondingly, ϕ_p is the value for a general variable at the center cell and ϕ_{nb} represent the one at the center of the neighboring cell. In this study, the scaled residual is observed to reach a constant of about $1e-12 \sim 1e-15$, which varies with the grids.

RESULTS AND DISCUSSION

(1) Grid convergence

First the convergence patterns are shown (Figure 3) with grid refinement for the calculated velocity at the points -- $(0, 1.1)$ and $(4, 0.1)$. Two types of grid convergence are identified namely – monotonic and oscillatory. It is also seen that the results are far from being grid independent. These figures illustrate that in the assumption of being in the asymptotic range is still a problem even with seven set of grids.

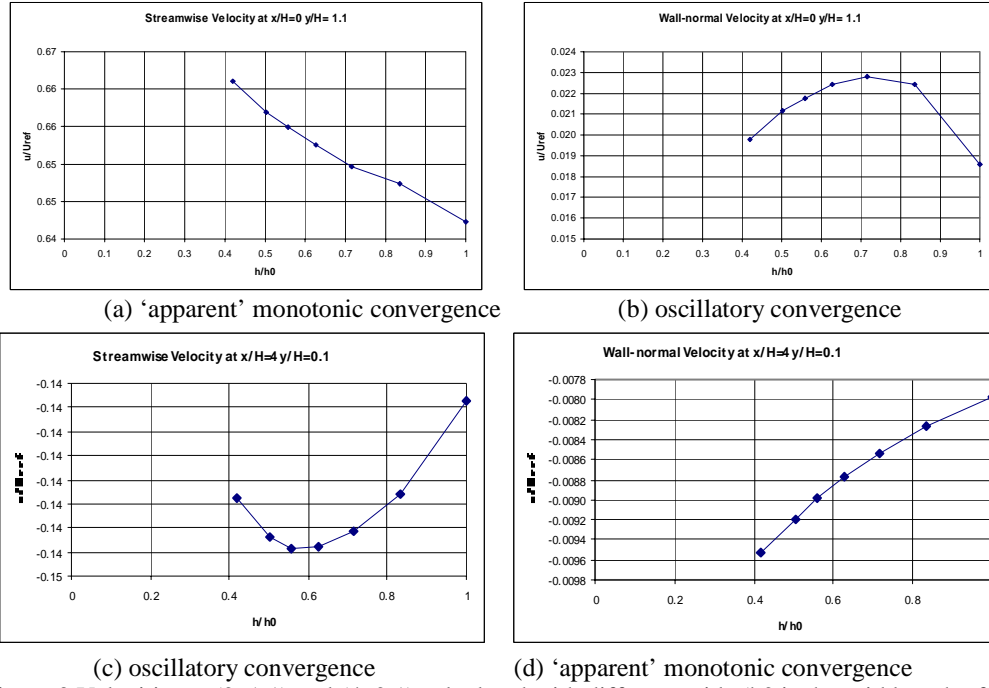


Figure 3 Velocities at (0, 1.1) and (4, 0.1) calculated with different grids (h_0 is the grid length of the coarsest grid)

(2) Least squares extrapolation

The results in Table 2&3 are calculated with least squares method using all 7 sets of grids. Uncertainty is estimated by using the Grid Convergence Index from Eq. (1).

Table 2 local flow quantities extrapolated with 7 sets of grids

Variable	$x=0, y=1.1h$	$x=h, y=0.1h$	$x=4h, y=0.1h$
U	6.619E-01	-1.952E-01	-1.442E-01
Uncertainty U	1.7E-03	1.51E-03	2.2E-02
Observed p	1.92	3.00	3.40
V	2.208E-02	1.426E-02	-9.289E-03
Uncertainty V	1.5E-01	7.15E-02	3.1E-02
Observed p	3.23	2.83	3.06
C_p	-1.727E-01	-2.421E-01	-1.164E-01
Uncertainty C_p	1.1E-01	2.26E-03	9.7E-03
Observed p	1.19	2.95	1.33
v_t	1.439E-03	1.192E-03	2.177E-03
Uncertainty v_t	3.9E-04	3.31E-03	4.3E-03
Observed p	3.07	3.06	3.07

Reattachment point: 6.203

Uncertainty: 4.6E-2

Observed p: 0.86

Table 3 Integral quantities extrapolated with 7 sets of grids

Flow quantity	Predicted	Uncertainty	Observed p
Friction resistance bottom wall(N)	2.640E-02	2.1E-03	3.07
Friction resistance top wall(N)	4.882E-02	2.0E-04	3.06
Pressure resistance bottom wall(N)	1.115E-01	5.6E-03	2.98

The results in Table 4&5 are calculated using least squares method with 4 sets of grids—101x101, 141x141, 181x181, 241x241. This is done because of two reasons: 1) Calculations with seven sets of grids are too many and unrealistic; 2) the grid refinement ratio with the set of seven is too small. Here also, uncertainty is estimated by using the Grid Convergence Index.

Table 4 local flow quantities extrapolated with 4 sets of grids

Variable	x=0,y=1.1h	x=h,y=0.1h	x=4h,y=0.1h
U	6.629E-01	-1.953E-01	-1.439E-01
Uncertainty U	3.5E-03	4.6E-04	1.9E-02
Observed p	1.96	3.14	3.37
V	2.176E-02	1.435E-02	-9.316E-03
Uncertainty V	1.3E-01	6.3E-02	2.7E-02
Observed p	3.21	3.05	3.17
C _p	-1.654E-01	-2.421E-01	-1.196E-01
Uncertainty C _p	5.0E-02	2.3E-03	2.4E-02
Observed p	1.60	3.11	2.59
v _t	1.440E-03	1.193E-03	2.177E-03
Uncertainty v _t	1.2E-03	2.2E-03	4.1E-03
Observed p	3.18	3.18	3.18

Reattachment point: 6.215

Uncertainty: 4.4E-2

Observed p: 0.89

Table 5 Integral quantities extrapolated with 4 sets of grids

Flow quantity	Predicted	Uncertainty	Observed p
Friction resistance bottom wall(N)	2.641E-02	2.0E-03	3.18
Friction resistance top wall(N)	4.883E-02	1.6E-04	3.18
Pressure resistance bottom wall(N)	1.115E-01	5.1E-03	3.12

The extrapolated quantities and the uncertainties predicted with 4 sets of grids are very close to the ones predicted with 7 sets of grids. Since 4 sets of grids are the minimum which least squares approach requires. This seems to be adequate for uncertainty analysis. Of the uncertainties at three different location (0, 1), (1, 0.1), and (4, 0.1), the ones at (1, 0.1) are the largest which may be caused by the rapidly changing of the flow field in that region. The observed p scatters in the range of 0.86 ~ 3.40 and it is difficult to identify the theoretical order of accuracy directly from these results. Positive observation is that the least squares method does not lead to unrealistically low (i.e. 0.1) or high (i.e. 10) observed order of accuracy.

(3) Extrapolation with methods using triplets

The quantities extrapolated with power law, AES, cubic spline, and polynomial method (See appendix for explanation on these methods) are compared to those calculated with least squares method as shown in Table 6. When oscillatory convergence happens, the extrapolated values predicted with the AES method are closest to the results with the least squares method. The GCI and the CV are compared in Table 7. It is seen that the CV predicted with the least squares method is much smaller than the ones calculated using the other methods with only 3 sets of grids. The GCI and CV normalized by the maximum in each row of Table 7 are then plotted in Figure 4. With the least squares method, the uncertainty calculated with the CV shows more consistence than the one with the GCI. Among these methods with triplets, the uncertainty associated with the power law seems to be much larger than the others. It remains to be seen which of these represent the unknown ‘reality’.

Table 6 Extrapolated quantities with different method

		Least squares(7 grids)	Least squares(4 grids)	Power Law	AES	Cubic spline	Polynomial
x=0 y=1.1	U	6.619E-01	6.629E-01	6.883E-01	6.586E-01	6.771E-01	6.837E-01
	V	2.208E-02	2.176E-02	1.231E-02	2.040E-02	1.533E-02	3.777E-03
	Cp	-1.727E-01	-1.654E-01	-2.047E-01	-1.515E-01	-1.857E-01	-1.982E-01
	v _t	1.439E-03	1.440E-03	1.419E-03	1.439E-03	1.428E-03	1.420E-03
x=1 y=0.1	U	-1.952E-01	-1.953E-01	-1.758E-01	-1.965E-01	-1.840E-01	-1.915E-01
	V	1.426E-02	1.435E-02	2.301E-02	1.453E-02	1.977E-02	2.231E-02
	Cp	-2.421E-01	-2.421E-01	-2.273E-01	-2.426E-01	-2.333E-01	-2.352E-01
	v _t	1.192E-03	1.193E-03	1.065E-03	1.203E-03	1.119E-03	1.174E-03
x=4 y=0.1	U	-1.442E-01	-1.439E-01	-1.379E-01	-1.424E-01	-1.393E-01	-1.265E-01
	V	-9.289E-03	-9.316E-03	-1.193E-02	-9.345E-03	-1.094E-02	-1.165E-02
	Cp	-1.164E-01	-1.196E-01	-1.001E-01	-1.187E-01	-1.071E-01	-9.552E-02
	v _t	2.177E-03	2.177E-03	2.320E-03	2.176E-03	2.263E-03	2.275E-03
	f(South)	2.640E-02	2.641E-02	2.750E-02	2.638E-02	2.706E-02	2.704E-02
	p(south)	1.115E-01	1.115E-01	9.967E-02	1.118E-01	1.044E-01	1.048E-01
	f(north)	4.882E-02	4.883E-02	4.865E-02	4.884E-02	4.873E-02	4.883E-02
	reattachment	6.203E+00	6.215E+00	5.992E+00	6.476E+00	6.177E+00	6.054E+00
	separation	8.988E-01	8.936E-01	1.039E+00	8.018E-01	9.470E-01	9.869E-01

Oscillatory convergence happens when refining the grids

Table 7 GCI and Coefficient of variation in quantities found by extrapolation in Table 6

		Least square				Power law	AES	Cubic spline	Polynomial
		GCI (7grids)	GCI (4 grids)	CV (7 grids)	CV (4 grids)	CV	CV	CV	CV
x=0 y=1.1	u	1.7E-03	3.5E-03	2.7E-03	4.8E-03	2.6E-02	1.2E-02	4.3E-03	1.0E-02
	v	1.5E-01	1.3E-01	7.9E-02	1.3E-01	4.2E-01	7.5E-02	5.6E-01	1.4E+00
	cp	1.1E-01	5.0E-02	2.6E-02	3.9E-02	1.5E-01	9.8E-02	5.6E-02	5.5E-02
	vis	3.9E-04	1.2E-03	5.1E-03	5.0E-03	2.1E-02	1.2E-02	3.4E-02	4.8E-02
x=1 y=0.1	u	1.5E-03	4.6E-04	5.2E-03	8.9E-03	8.0E-02	4.2E-02	2.1E-02	5.7E-02
	v	7.1E-02	6.3E-02	5.8E-02	1.0E-01	2.2E-01	1.5E-01	5.8E-02	7.9E-02
	cp	2.3E-03	2.3E-03	4.1E-03	7.2E-03	4.3E-02	2.1E-02	5.4E-03	2.6E-02
	vis	3.3E-03	2.2E-03	5.3E-03	8.9E-03	8.6E-02	4.4E-02	3.1E-02	6.4E-02
x=4 y=0.1	u	2.2E-02	1.9E-02	9.1E-03	1.6E-02	4.4E-02	1.3E-02	4.2E-02	5.3E-02
	v	3.1E-02	2.7E-02	2.8E-02	4.7E-02	1.3E-01	7.5E-02	3.3E-02	4.3E-02
	cp	9.7E-03	2.4E-02	1.6E-02	3.1E-02	1.2E-01	3.2E-02	5.2E-02	3.2E-02
	vis	4.3E-03	4.1E-03	5.8E-03	9.9E-03	4.0E-02	2.3E-02	1.1E-02	2.2E-02
	f(South)	2.1E-03	2.0E-03	3.2E-03	5.5E-03	2.6E-02	1.4E-02	3.4E-04	1.4E-02
	p(south)	5.6E-03	5.1E-03	7.8E-03	1.4E-02	7.6E-02	3.6E-02	2.0E-03	4.0E-02
	f(north)	2.0E-04	1.6E-04	1.5E-04	2.1E-04	2.5E-03	1.4E-03	1.9E-03	2.8E-03
	reattachment	4.6E-02	4.4E-02	2.6E-03	4.6E-03	4.9E-02	2.1E-02	1.0E-02	1.6E-02
	separation	1.3E-01	1.2E-01	7.9E-03	1.4E-02	1.4E-01	8.6E-02	2.1E-02	5.9E-02

Oscillatory convergence happens when refining the grids

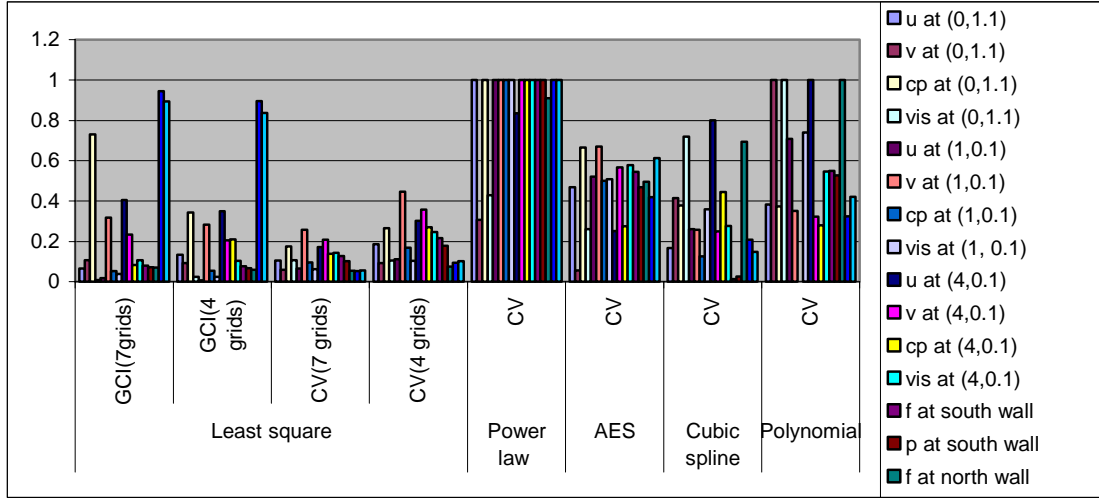


Figure 4 Normalized GCI and CV with different methods and different cases

When presenting results from a CFD application it is usually desirable to present calculated field variables with error bars in terms of profiles at certain locations in parallel with experimental results. Figure 5 and 6 depicts the normalized error in the streamwise velocity component at $x/H = 1$ as a function of vertical distance y/H . It is seen that extrapolation using power law is problematic, especially in the region where oscillatory convergence is present. When an average value is used for the observed order i.e.

$$p_{ave} = \sum_{k=1}^N p_k, N \text{ being the number of data points, the results obtained from power law are in concert with}$$

the other methods (see Fig. 6) where the calculation of p is not an issue. We suspect that the ‘truth’ is somewhere among the four cases shown in Fig. 6. But it remains to be seen which one of these results in Fig. 5 represents the ‘truth’.

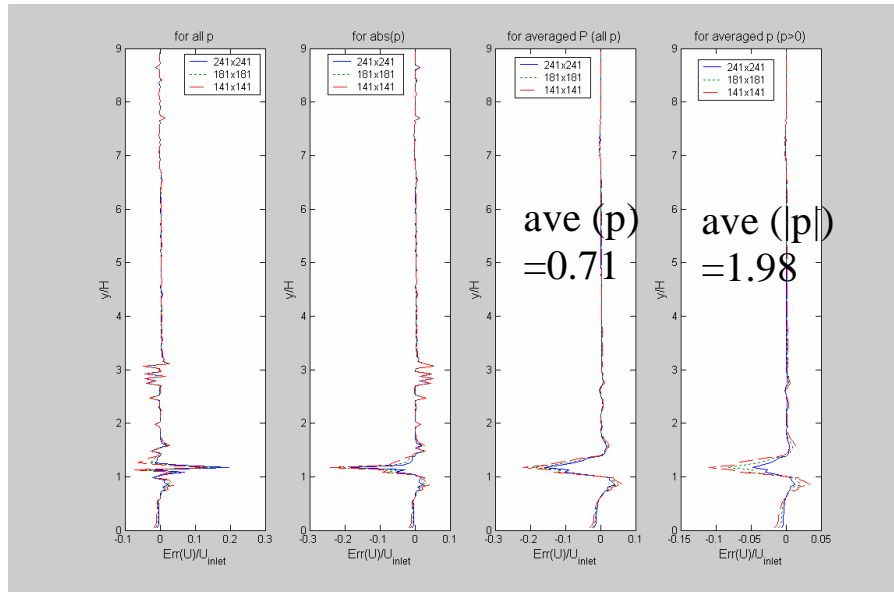


Figure 5 Extrapolated streamwise velocity profile using power law with different ways handling the power p

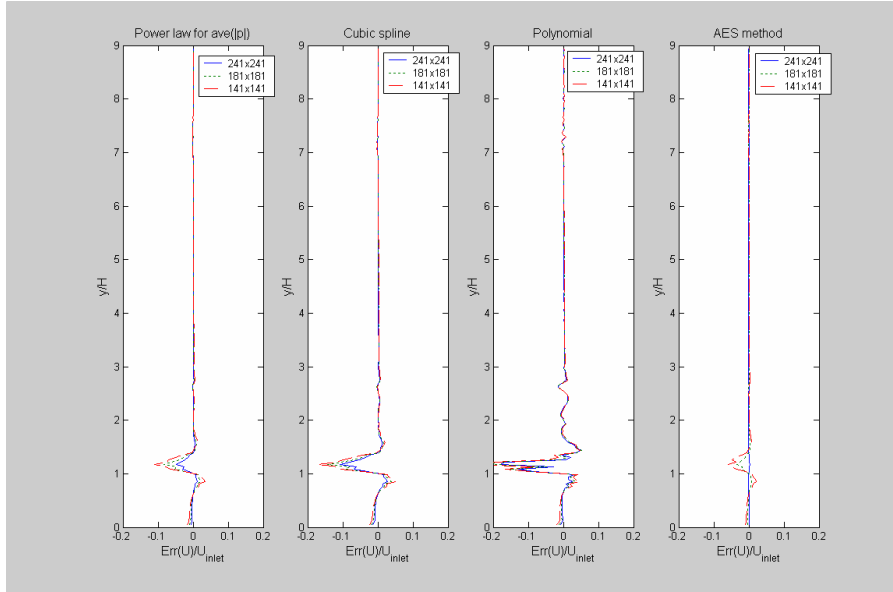


Figure 6 Comparison of the extrapolated streamwise velocity profile at $x/H=1$ with different methods

(4) Results with no interpolation

The separation and reattachment lengths calculated with doubling rectangular grids are shown in Table 8. This grid doubling is done to avoid interpolation. Again, the oscillatory convergence is observed for the reattachment length calculated with rectangular grids. The extrapolated quantities and coefficients of variation are listed in Table 9. Among the coefficients of variation for all methods, the ones with the least squares method exhibit the smallest variation.

Comparison of Table 7 and Table 9 show that the extrapolated reattachment length is in general significantly smaller (by about 7%) when the rectangular grids are used with grid doubling. On the other hand, the uncertainty indicated by coefficient of variation is larger when interpolation errors are minimized.

The streamwise velocity component at (1.01, 0.125) with different grids are shown in Table 10. The velocities calculated with the rectangular grids and with no interpolation are shown on the left two columns. On the right, the velocities are computed with the non-rectangular grids and with the bilinear interpolation method. The extrapolations are performed by using least squares method as shown in Table 11. It is seen first that the extrapolated velocity with rectangular grids are somewhat different from the ones with non-rectangular grid. It is also observed that the numerical uncertainty (GCI and CV) calculated with the rectangular grids are quite smaller than the ones with the non-rectangular grids. The apparent order of accuracy, p , with rectangular grids is closer to the theoretical order used in this study.

CONCLUSIONS

This extensive effort on analysis of grid convergence and the estimation of numerical uncertainty has shown that when calculations are repeated on significantly different set of four grids, the least squares method gave results that seem to be at least consistent among themselves. We obtained very similar results using 7 sets of grids and 4 sets of grids, hence four sets of carefully selected grids should be adequate for uncertainty analysis. The major problem again, seems to arise from cases that exhibit oscillatory convergence. In fact, it may be erroneous to assume monotonic convergence just by observing the behavior of three or four points. In this regards, it may be necessary to devise methods which perform well both for monotonic, and oscillatory cases. Some of methods are proposed in this category has shown potential to predict the extrapolated values and the variance in that without specifically employing the observed order.

In particular, the approximate error spline method when used with triplets among four sets of grids may be a good choice to estimate the mean extrapolated values and the variance in that mean.

It remains to be seen if these conclusions will hold even after the conference when all results from different groups are compared with each other.

Table 8 Quantities calculated with Cartesian grids and non-interpolation

	61*61	121*121	241*241	481*481
Separation point	0.0605	0.3143	0.7174	0.8026
Reattachment point	5.5277	5.7498	5.6752	5.8353

Table 9 Extrapolated quantities and coefficients of variation
(Values in Parenthesis are from Table 6 & 7)

	Separation point		Reattachment point	
	Mean	CV	Mean	CV
Least squares	1.19 (0.89)	6.7E-02 (1.4E-02)	5.77 (6.22)	1.4E-02 (4.6E-03)
Power law	1.39	3.2E-01	5.82	8.9E-02
AES	0.73	1.3E-01	5.75	1.8E-02
Cubic spline	1.00	1.5E-01	5.80	5.0E-02
Polynomial	1.06	2.7E-01	5.80	8.4E-02

Table 10 Streamwise velocity at (1.01, 0.125) calculated with different grids

Rectangular grids	velocity with no interpolation	non-rectangular grids	velocity with interpolation
61*61	-2.0340E-01	101*101	-2.0360E-01
121*121	-1.9132E-01	121*121	-1.9647E-01
241*241	-1.8979E-01	141*141	-1.9210E-01
481*481	-1.8865E-01	161*161	-1.8916E-01
		181*181	-1.8724E-01
		201*201	-1.8593E-01
		241*241	-1.8433E-01

Table 11 Extrapolated streamwise velocity at (1.01, 0.125) with least squares method

	non-rectangular		rectangular
	7 sets of grids	4 sets of grids	4 sets of grids
U	-0.1840	-0.1842	-0.1887
GCI	2.0E-03	1.0E-03	2.0E-04
p	3.004	3.146	2.272
CV	5.0E-03	8.6E-03	3.4E-03

REFERENCES

- Cadafalch, J., Perez-Segarra, C.D., Consul, R. and Oliva, A. (2002) "Verification of Finite Volume Computations on Steady-State Fluid Flow and Heat Transfer," ASME Journal of Fluids Engineering, Vol. 124, pp.11-21.
- Celik, I., Chen, C.J., Roache, P.J. and Scheurer, G. Editors. (1993), "Quantification of Uncertainty in Computational Fluid Dynamics," ASME Publ. No. FED-Vol. 158, ASME Fluids Engineering Division Summer Meeting, Washington, DC, 20-24 June.

- Celik, I. and Zhang, W-M (1993) "Applicaton of Richardson Extrapolation to Some Simple Turbulent Flow Calculations," Proceedings of the Symposium on "Quantification of Uncertainty in Computational Fluid Dynamics," Editors: I. Celik et al. ASME Fluids Engineering Division Spring Meeting, Washington, C.C., June 20-24, pp. 29-38.
- Celik, I. and Karatekin, O. (1997), "Numerical Experiments on Application of Richardson Extrapolation with Nonuniform Grids," ASME Journal of Fluids Engineering, Vol. 119, pp.584-590.
- Celik, I., Li, J., Hu, G., and Shaffer, C. (2004) "Limitations of Richardson Extrapolation and Possible Remedies for Estimation of Discretization Error" Proceedings of HT-FED2004, 2004 ASME Heat Transfer/Fluids Engineering Summer Conference, July 11-15, 2004, Charlotte, North Carolina USA, HT-FED2004-56035
- Eca, L. and Hoekstra, M. (2002), "An Evaluation of Verification Procedures for CFD Applications," 24th Symposium on Naval Hydrodynamics, Fukuoka, Japan, 8-13 July.
- Eca, L. and Hoekstra, M. (2003), "Uncertainty Estimation :A Grand Challenge for Numerical Ship Hydrodynamics" 6th Numerical Towing Tank Symposium, Rome, September 2003
- Eca, L. et al., (2004) "Workshop on Numerical Uncertainty Estimation" Lisbon, Portugal 2004
- FLUENT company 2004 FLUENT 6.0 User Reference Manual
- Phillips, G.M. and Taylor, P.J. (1973) "Theory and Applications of Numerical Analysis" Academic Press: London and New York, pp.345
- Richardson, L.F. (1910) "The Approximate Arithmetical Solution by Finite Differences of Physical Problems Involving Differential Equations, with an Application to the Stresses In a Masonary Dam," Transactions of the Royal Society of London, Ser. A, Vol. 210, pp. 307-357.
- Richardson L.F. and Gaunt, J. A. (1927) "The Deferred Approach to the Limit," Philos. Trans. R. Soc. London Ser. A, Vol. 226, pp. 299-361.
- Roache, P.J.(1998) "Verification and Validation in Computational Science and Engineering," Hermosa Publishers, Albuquerque
- Stern, F., Wilson, R. V., Coleman, H. W., and Paterson, E. G. (2001), "Comprehensive Approach to Verification and Validation of CFD Simulations - Part 1: Methodology and Procedures," ASME Journal of Fluids Engineering, Vol. 123, pp. 793-802, December.

APPENDIX

(1) Least squares method

With the least squares approach, we compute ϕ_0 , α , and p by minimizing the following function.

$$S(\phi_0, \alpha, p) = \sqrt{\sum_{i=1}^n (\phi_i - \phi_0 - \alpha h_i^p)^2} \quad (1.1)$$

where n is the number of grids available. The minimum of (1.1) is found by setting the derivatives of (1.1) with respect to ϕ_0 , α , and p equal to zero, which leads to a non-linear system of equations. Solving the non-linear system yields values for ϕ_0 , α , and p.

(2) Polynomial method

This method uses the first few terms in the Taylor expansion of $\phi(h)$ to approximate $\phi(h)$. For instance, assuming the method is first-order, we can use the first three terms if we have 3 sets of grids. That is

$$\phi(h) = \phi(0) + a_1 h + a_2 h^2 \quad (2.1)$$

If we have 4 sets of grids, we can use

$$\phi(h) = \phi(0) + a_1 h + a_2 h^2 + a_3 h^3 \quad (2.2)$$

If the scheme is higher order ($p \geq 2$), this method will mean essentially a curve fit to the actual error function. For a fourth order method one has to keep at least 4 terms, i.e. five sets of calculations are needed.

The extrapolation to the limit approach is recommended to solve the equations formed by polynomial method. This approach uses the following formula to calculate the extrapolated solution $\phi^{(3)}(h)$ for 3 sets of grids and $\phi^{(4)}(h)$ for 4 sets of grids.

$$\phi^{(m)}(h) = \frac{\phi^{(m-1)}(\alpha h) - \alpha^m \phi^{(m-1)}(h)}{1 - \alpha^m} \quad m=1, 2, \dots \quad (2.3)$$

It's easy to tabulate the sequential steps of the calculation procedure and to add more points later.

(3) Power law method

We use the Power law method proposed by Celik and Karatekin(1997) for 3 sets of grids. The idea follows

$$\phi(0) - \phi(h_1) = ch_1^p \quad (3.1)$$

$$\phi(0) - \phi(h_2) = \text{sign}\left(\frac{\varepsilon_{32}}{\varepsilon_{21}}\right) ch_2^p \quad (3.2)$$

$$\phi(0) - \phi(h_3) = ch_3^p \quad (3.3)$$

where $\varepsilon_{32}/\varepsilon_{21} = (\phi(h_3) - \phi(h_2))/(\phi(h_2) - \phi(h_1))$ the sign of which is positive for monotonic convergence and negative for oscillatory convergence. There are 3 unknowns, $\phi(0)$, c, and p. We can implement the same iterative method to solve (3.1)-(3.3) as done by Celik and Karatekin (1997).

For 4 sets of grids, we can apply

$$\phi(h_i) - \phi(0) = a_1 h_i^p + a_2 h_i^{p+1} \quad i = 1, 2, 3, 4 \quad (3.4)$$

Oscillatory convergence is facilitated if a_1 and a_2 are of opposite sign. It should be noted that for some cases there is no solution to Eq. (3.4). Those cases will be counted as unsuccessful outcomes.

(4) Cubic spline method

The well known natural cubic splines curve fitting technique is used to create the cubic splines between three points or four points. $\phi(0)$ can be found by extrapolating the curve for the interval closest to $h=0$.

(5) Approximate error spline method

Still using Taylor series expansion for $\phi(h)$ and substituting αh for h , we have

$$\phi(\alpha h) = \phi(0) + a_1 \alpha h + a_2 (\alpha h)^2 + a_3 (\alpha h)^3 + \dots \quad (5.1)$$

The true error E_t is given by

$$E_t(\alpha, h) \equiv \phi(\alpha h) - \phi(h) = \sum_{k=1}^{\infty} a_k \alpha^k h^k \quad (5.1)$$

and the approximate error E_a

$$E_a(\alpha, h) \equiv \phi(\alpha h) - \phi(h) \quad (5.2)$$

where $E_t(\alpha, h)$ is the true error and $E_a(\alpha, h)$ is the approximate error which presents the difference of the subsequent results with the fine grid and the coarse grid. So we have

$$E_a(\alpha, h) = \sum_{k=1}^{\infty} a_k (\alpha^k - 1) h^k \quad (5.3)$$

Dividing (5.1) by (5.3) and moving $E_a(\alpha, h)$ to the right hand side yield

$$E_t(\alpha, h) = \frac{1}{1 - \frac{\sum a_k h^k}{\sum a_k \alpha^k h^k}} E_a(\alpha, h) \quad (5.4)$$

letting

$$\frac{\sum a_k h^k}{\sum a_k \alpha^k h^k} = b_0 + b_1 h + b_2 h^2 \quad (5.5)$$

and expanding the l.h.s. of the above equation and comparing it with the r.h.s. give

$$\begin{aligned} b_0 &= \frac{1}{\alpha} & b_1 &= \left(\frac{1-\alpha}{\alpha} \right) \frac{a_2}{a_1} \\ b_2 &= \left(\frac{1-\alpha^2}{\alpha} \right) \frac{a_3}{a_1} - (1-\alpha) \left(\frac{a_2}{a_1} \right)^2 \end{aligned} \quad (5.6)$$

Now Eq. (5.4) can be rewritten as

$$E_t(\alpha, h) = \frac{1}{1 - (b_0 + b_1 h + b_2 h^2)} E_a(\alpha, h) \quad (5.7)$$

In order to calculate b_0, b_1 & b_2 , we need to calculate $a_1, a_2, \& a_3$ first. It is seen from Eq. (5.3) that

$$a_k = \frac{E_a^{(k)}(\alpha, 0)}{k! (\alpha^k - 1)} \quad k = 1, 2, 3 \quad (5.8)$$

$E^{(k)}$ is the k^{th} derivative of E . Assuming that we have 3 sets of grids and the solutions as $(h_1, \phi(h_1))$, $(h_2, \phi(h_2))$ and $(h_3, \phi(h_3))$ with $h_3 = \alpha h_2 = \alpha^2 h_1$. And noting that $E_a(\alpha, 0) \equiv 0$ leads to 3 points as $(h_1, E_a(\alpha, h_1))$, $(h_2, E_a(\alpha, h_2))$ and $(0, E_a(\alpha, 0))$ which involves the approximate error instead of the numerical solution $\tilde{\phi}$ itself. Using the information on E_a we can interpolate with cubic splines using two endslopes given by $E_a'(\alpha, 0) \equiv 0$ and $E_a'(\alpha, h_1) \equiv (E_a(\alpha, h_1) - E_a(\alpha, h_2)) / (h_1 - h_2)$. These endslopes are acceptable at $h=0$ for any scheme with order larger than 1. For the first order methods, in general, the slope at $h=0$ is not zero. We could still obtain excellent results using the zero slope assumption for the first order methods as we demonstrate in the assessment part of this paper. Once we have $E_a^{(k)}(\alpha, 0)$, we can calculate a_k from Eq (5.8). As one might notice, b_1 is singular at $h=0$ if $E_a'(\alpha, 0) = 0$. In order to avoid this singularity, $E_a'(\alpha, \varepsilon)$ can be used to represent $E_a'(\alpha, 0)$ by using finite differencing at $h = \varepsilon$ where ε is a small value. Having obtained b_0, b_1 and b_2 , we can calculate $\phi(0)$ from Eq. (5.7) together with the definition (5.1) and (5.2).